DEVELOPMENT OF TWO-WAY COUPLED CFD – DEM MODEL FOR TOP SPRAY FLUID BED GRANULATOR USING STAR CCM+

By

DHEERAJ REDDY DEVARAMPALLY

A thesis submitted to the

Graduate School-New Brunswick

Rutgers, The State University of New Jersey

In partial fulfillment of the requirements

For the degree of

Master of Science

Graduate Program in Chemical and Biochemical Engineering

Written under the direction of

Dr. Rohit Ramachandran

And approved by

_____

_____

_____

_____

New Brunswick, New Jersey

May, 2017

Abstract of the Thesis

Development of Two-way Coupled CFD - DEM Model for Top Spray Fluid Bed Granulator Using STAR-CCM+

by **Dheeraj Reddy Devarampally**

Thesis Director: Dr. Rohit Ramachandran

A two-way coupled Computational fluid dynamics (CFD) – Discrete element method (DEM) model is developed using STAR-CCM+ for a top spray fluid bed granulator to study the effects of process parameters such as inlet air flow rate, temperature on the particle dynamics and the residence time in the spray zone. The framework relies on coupled CFD–DEM simulations to provide particle-level mechanistic information such as collision frequencies, particle flux and residence time of the particles in the spray zone. Particles of diameter 1 mm (Group B particles according to Geldart's classification of powders) are considered for model development. To reduce the computational load, the particles are scaled by keeping the non-dimensional terms Archimedes, Reynolds's numbers and the minimum fluidization velocity of the system constant. Passive scalar model is also used for Lagrangian phase to track the residence time of the particles within the spray zone. This model accurately predicts the effect of process parameters (inlet air flow rate, temperature) on the particle dynamics and the particle residence time inside the spray zone. This mechanistic data can be used in Population balance models (PBM) to model the rate processes such as agglomeration, breakage and consolidation.

Acknowledgements

I would like to thank my thesis adviser Dr. Rohit Ramachandran for providing me the opportunity to work in the Particulate systems lab group and mentoring me along the process. Thank you Dr. Benjamin Glasser and Dr. Ravendra Singh for taking time to be on my thesis committee. I would like to thank Ashu Tamrakar for his help throughout the project and for all the discussions that led to the successful completion of this project.

Special thanks to the team at particulate systems lab Chandra kanth Bandi, Anik Chaturbedi, Sheng –Wen Chen, Subhodh Karkala and Shashank Muddu, it was great working with every one of you. Thanks to my friends Siddharth Singh, Suparna Rao, Sri Swaroop Dasari, Venkat Neehar and Shashank kosuri for all your support in making the stay at Rutgers a memorable one.

Finally, I would like to thank my parents, sister and cousins for being there for me and supporting me through every step of my life.

Table of contents

List of tables

List of figures

1. Introduction

Granulation is a size enlargement process where small/fine powder particles are converted into granules to address issues such as poor flow, handling, segregation and poor dissolution of powders. The two most widely used granulation types in pharmaceutical industries are Wet and Dry granulation. Wet granulation is where liquid binder is added to the powder. It can be accomplished using different types of equipment such as high shear granulator, fluid – bed granulator, twin- screw granulator and drum granulators. Fluid – bed granulation is widely used as the dry mixing, wetting of the blend and drying of the granules can be achieved in a single operation which helps avoid transfer losses, labor costs and time (Burggraeve et al., 2013). Fluid bed granulators also provide good heat transfer and mixing, control over granule morphology and are easy to scale up which is advantageous when compared to other granulators. But the cost of operating fluid beds are usually high and they cannot handle fine powders as they cannot be fluidized (Geldart, 1973).

The Food and Drug Administration (FDA) guidelines encourage the pharmaceutical industry to take the Quality by Design approach which advocates that the quality should be built into the product. FDA's Process Analytical technology (PAT) initiative calls for the use of real time monitoring of unit operations for a better control of product quality (Burggraeve et al., 2013). To monitor the processes in real time, models that predict the product quality based on the process parameters should be developed. Predictive models that link critical process parameters (CPP's) and formulation parameters to critical quality attributes (CQA's) can be used to understand/capture the process dynamics. The need to develop mechanistic understanding of granulation process also stems from the necessity to make the existing manufacturing processes cost effective and run faster - especially in the ever-increasing research and development cost landscape. According to Gernaey et al.

(Gernaey et al., 2012) there are two ways to maximize the profits, particularly in pharmaceutical industry (a) Rapid process development to prolong the patent life of a product and (b) Optimizing the production processes which would then allow companies to compete with generic drug manufacturers after the patent expiration. Use of process modeling can help achieve these goals. The use of process modeling becomes especially relevant here since empirical studies of granulation which depends on a number of parameters would require a large set of experiments which are impractical to perform (in terms of cost and time). Multi-scale and multi-phase models can carry out virtual experimentation and can be used for design space exploration; would therefore speed up the process development and scale-up of unit operations.

Along the spectrum of modeling approaches, mechanistic models based on the fundamental physics of the system are at one extreme which would capture detailed process behavior (Cameron et al., 2005). On the other end, there are empirical models which use experimental data and fit suitable models to it. To develop a first-principal based model for a fluid-bed granulation process, it is important to model the fluid – particle interaction. Computational fluid dynamics (CFD) is used to model the continuous phase (air) flow behavior. CFD solves the volume averaged conservation of mass, momentum and energy equations over discretized domain. Discrete element methods (DEM) is used to model the discrete phase (particles/solids), which applies equations of motion, conservation of momentum and energy equations to each particle in the system. A transfer of momentum, mass and energy should be established between CFD and DEM to model the interactions between the fluid –particle and vice-versa. In systems which contain low solid volumes, a one-way coupling is good enough which only transfers the data from CFD to DEM i.e. the fluid flow affects the particle motion but the particles are not responsible for fluid flow. Fluid bed granulators contains high solid volumes, so the particle's effect on the fluid flow cannot be ignored. The mechanistic data such as collision

frequencies, residence times and particle flux can be used in a Population balance model (PBM) to describe the aggregation, breakage and consolidation mechanisms that occur during granulation and model the changes in particle size and properties. The framework described in the current work operates on different length scales, DEM describes the process on a particle level (micro-scale) and CFD describes the continuous phase over a discretized region (macro-scale).

1.1 Objectives

- Develop a two-way coupled CFD –DEM model for a top-spray fluid bed granulator using STAR-CCM+.
- Study the effect of inlet air flow rate and temperature on the particle dynamics.
- Study the effect of inlet air flow rate on the particle residence times inside the spray zone.

2. Background

2.1 Computational fluid dynamics (CFD)

Computational Fluid Dynamics (CFD) has been widely used in chemical industry to model internal and external fluid flows. CFD has been used to optimize processes, reduce the energy costs and create new designs without wasting resources by performing experiments. In pharmaceutical industry, CFD can be used to model fluid flow in several processes such as Mixing, separation, and fluidized bed granulators (Lyngberg et al., 2016). Computational fluid dynamics calculate the fluid flow field by solving the volume averaged Navier – Stokes, energy and species conservation equations over the discretized region. CFD models fluid and particles using Eulerian – Eulerian approach, assuming fluid and particles as continuum phases. This approach only accurately models fluid but not the particles as the particles are a dispersed phase rather than a continuous one. To accurately model the particles, discrete element modeling is used which uses a lagrangian approach to track the particles in space and time.

The use of CFD provides a distinct advantage of solving the velocity, pressure and temperature profiles of the fluid over the desired domain. This is done by discretizing the entire region of interest into cells and volume averaged conservation equations of mass, momentum, species and energy are solved over this region. Due to the large number of discretized cells in a given region, CFD is often computationally expensive. The accuracy of the solution generally increases with increase in cells in region, but using a smaller grid size to discretize the region results in longer computational time. Most commercial CFD software such as STAR-CCM+ from CD-Adapco, ANSYS Fluent and other open source software provide parallel computing options to speed up the computational processes.

Fluid bed granulation is a multiphase system with fluid phase and solid phase interacting with each other. The flow of one phase affects the flow of the other phase. As mentioned above, CFD uses Eulerian-Eulerian approach to model fluid – particle interactions. To increase the particle level detail that is required in modeling this unit operation DEM is used in conjunction with CFD.

2.2 Discrete Element Method (DEM)

In high loading multiphase systems such as fluid beds, the particle-particle and particle-boundary interactions cannot be ignored (Cd-Adapco, 2016). To resolve the effects of these interactions on individual particles, Newton's laws of motion and Euler's equations of rotational motion are solved for each individual particle(Sen et al., 2014). Discrete Element Method (DEM) is a numerical method that resolves the motion of individual solid particles.

In this current model developed a soft sphere DEM approach has been used, where the particles are allowed to overlap and the extent of overlap is used to determine the contact forces (normal and tangential). In this approach, multiple particles can be in contact simultaneously and the contact time is finite (Cundall and Strack, 1979).

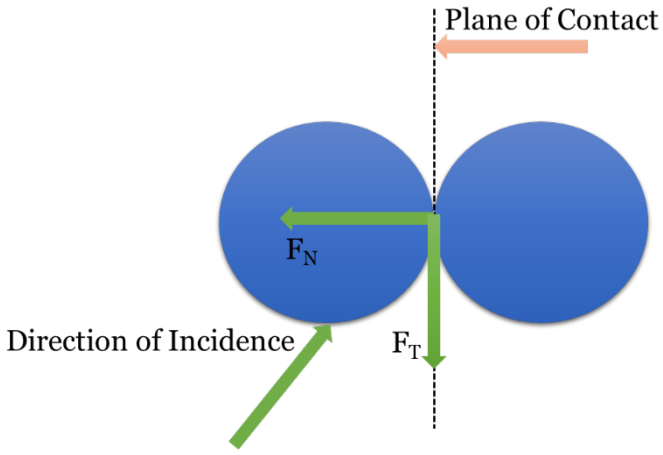

Figure 2.1. Contact between two soft spheres, the contact force is resolved into two components F_N (normal contact force) and F_T (Tangential contact force).

The interparticle contact forces are calculated by assuming that the particle-particle interaction as a spring-dashpot system with friction sliders. Models such as Hertz – Mindlin No-slip contact, linear spring and Walton Braun (Cd-Adapco, 2016) are used to calculate the normal and tangential components of the contact force. External forces on the particles such as gravity, cohesion and fluid forces are also added accordingly.

Discrete element method is computationally expensive as the method resolves the motion of individual particles in the system. A typical multiphase system such as fluid bed granulator has billions of particles and it is not practical to resolve the motion of all the particles in this system. In the current work scaling laws are used to reduce the number of particles in the system and thereby reducing the computational load.

2.3 Coupling CFD – DEM

Computational fluid dynamics and Discrete Element Method are coupled to capture the fundamental dynamics of the fluid-particle system. The coupling approach between CFD and DEM can either be done through a one-way data transfer or two-way data transfer. In one-way coupling, the fluid flow field calculated by CFD is exported and added as an external force on the particles in DEM simulation. Using this approach however ignores the effects of particle interactions on the fluid flow; hence, this approach is generally suitable for low solids volume applications like a cyclone separator. In two way coupling, the transfer of data between CFD and DEM goes both ways- there is an exchange of mass, momentum and velocity information between the solid phase and the fluid phase. The coupling process and the transfer of information is summarized in Figure 2.

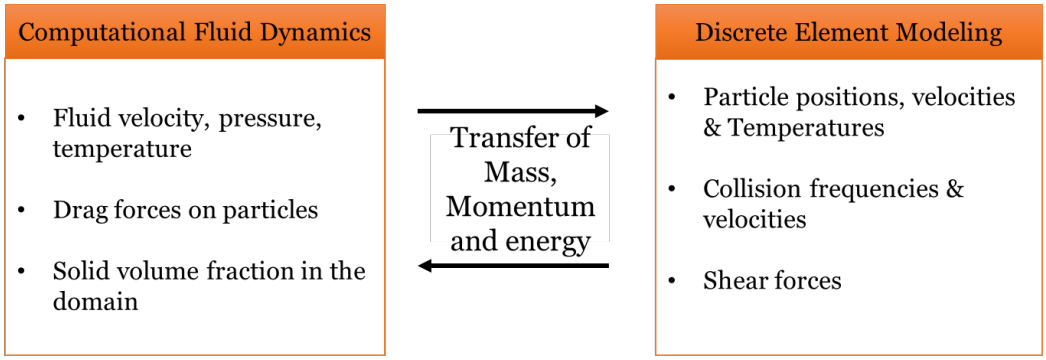

Figure 2.2. Data Transfer between CFD and DEM through Two - way coupling approah (Norouzi et al., 2016).

In the past two-fluid models have been used to model multiphase fluid – particle systems, which model both fluid and particles as continuous phases and resolves the conservation of mass, momentum and energy equations for both the phases [(Hoomans et al., 1996), (Ding Jianmin and Gidaspow, 1990), (Kuipers et al., 1993)]. As described in section 2.1, these models do not consider the discrete nature of the solid phase. Replacing the two-fluid model, a lagrangian multiphase model can be used which makes use of discrete element method to account for the discrete nature of particles.

Several authors have developed CFD-DEM models to study the fluidization phenomena. Yuu et al. (Yuu et al., 2000) modeled a fluid bed using 100,000 particles of 310 microns in diameter using Coupled CFD-DEM simulations to study the bubble formation, coalescence and disruption. The model accurately describes the hydrodynamic behavior of the particles in the experiments, obtained through instantaneous particle positions and velocities. Other authors have validated the CFD-DEM models of powder beds in different regimes with experimental results (Bokkers et al., 2004).

Fries et al. (Fries et al., 2011) have used coupled CFD-DEM studies to study the particle and fluid behavior in top spray fluid bed granulator and Wurster coater. Effect of process parameters such as fluid velocity, height of the Wurster tube in case of Wurster coater are also studied. The authors studied the residence time distributions of particles in the spray

zone in both the granulators and have found that the Wurster coater provides a narrow residence time distribution of particles inside the spray zone where as a wide distribution of residence time inside the spray zone has been obtain in case of a top spray fluid bed granulator. Which makes wetting in Wurster coater is more homogenous than that in a top spray fluid bed granulator due to its unstable flow structure.

In another study, Fries et al. (Fries et al., 2013) have studied the collision dynamics of the particles in different fluid bed granulators to measure the probability of agglomeration, breakage and also strength of the agglomerates and found that the Wurster coater is the best equipment to produce uniform, large and stable granules and the collision dynamics obtained from the numerical simulations corroborated the experimental results.

The models described above used the dynamics of particles in the fluid beds to study the effects on agglomeration. To comprehensively study the agglomeration of particles into granules, Sen et al. (Sen et al., 2014)used a hybrid CFD-DEM-PBM model. Similar to the models described above, Sen et al. used CFD-DEM model to describe the particle dynamics and extract critical data such as collision frequencies between particles of different sizes, circulation from the bottom of the fluid bed to the top. In addition to this, custom models are used within DEM model to simulate the addition of liquid binder and PBM is then used to model the aggregation of particles. However, the effect of process parameters such as inlet fluid velocity, breakage and consolidation of particles has not been studied by the authors.

3. Method Development

In this section simulation set up in STAR-CCM+ is presented.

3.1 Geometry, Meshing and Boundary types

3.1.1 Geometry:

The geometry of the system is modeled after top spray fluid bed granulator, GPCG 1 by Glatt (Wormsbecker et al., 2007). The geometry (Figure 3.1) was created using built in 3D-CAD module available in STAR-CCM+.

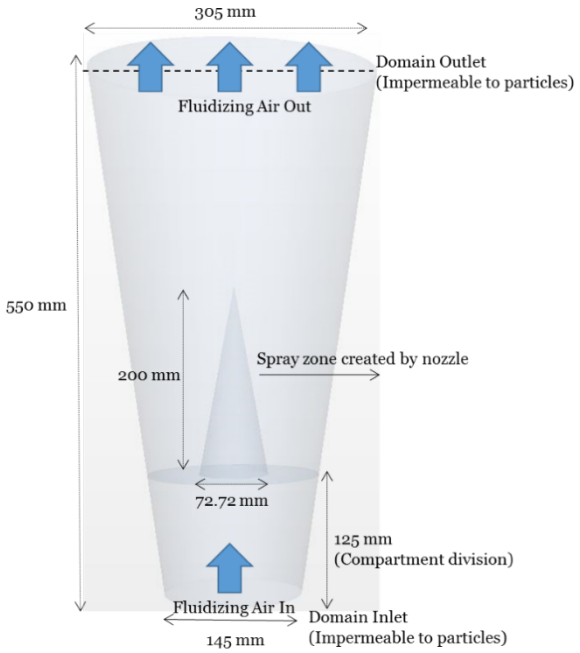

Figure 3.1. Geometry setup of GPCG 1

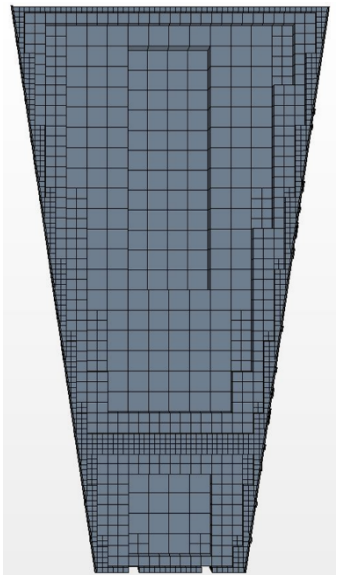

Figure 3.2. Internal Mesh of the domain.

A virtual geometry for the zone created by the spray nozzle (not meshed, used only to visualize) is constructed inside the GPCG 1 as shown in Figure 3.1, the approximate geometry of the spray zone is obtained from the high resolution image of the spray zone created by a two phase nozzle spraying water (Hao Chen et al. 2016). The dimensions of the spray zone are shown in the figure 3.3. The spray zone is located 5 mm above the

static bed height, this value can be changed by changing the position of the spray nozzle. The zone below the spray cone is designated as the bottom compartment and the rest of the geometry is designated as the top compartment. This is done for post – processing purposes, where the mechanistic data in the bottom and top compartment can be used in the compartmental population balance model to model the rate processes in granulation (Sen et al., 2014).

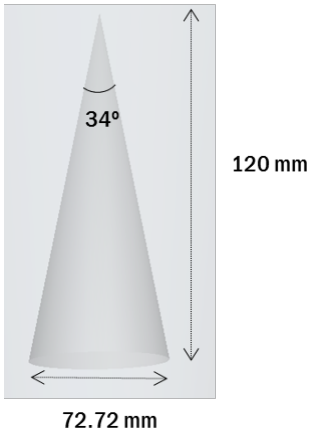

Figure 3.3. Shape of the spray zone created by the atomized liquid binder particles.

3.1.2 Mesh:

A Trimmer mesh with a base size of 5 mm has been used which creates cells as can be seen in figure 3.2. Trimmer mesh has created the minimum number of cells for the given base size of 5 mm among tetrahedral and polyhedral meshes available. A prism layer mesh is also added to the domain, which decreases the cell size at the walls for a better resolution of flow field at the walls. The mesh parameters and their values are presented in table 3.1.

Mesh parameter	Value
Total number of Cells	84830
Number of Interior Faces	246518
Number of vertices	98431

Table 3.1. Mesh parameters

3.1.3 Boundary Types:

The boundary types for this setup are presented in table 3.2. At every domain boundary, "boundary types" are set for each phase. For Domain inlet and outlet, the air is allowed to pass through the boundaries but not the particles, therefore a "phase impermeable" boundary condition is applied at the boundaries for the solid phase, which makes the inlet and the outlet of the domain act as walls with respect to the particles. The boundary condition at the domain walls is set to "Wall" for both the air and particles.

Boundary Types	
Domain Inlet	Air - Mass flow inlet Particle – Phase Impermeable
Domain Outlet	Air – Pressure Outlet Particle – Phase Impermeable
Domain Walls	Air – Wall (no-slip) Particle – Wall

Table 3.2. Domain boundary types

3.2 Physics Models used for the Fluid and Solid Phase

To compute the flow field of the continuous phase in a system, computational fluid dynamics solves set of discretized linear equations. As mentioned in section 2.1, CFD solves the volume averaged conservation equations in all the cells in the flow domain. To resolve the motion of the particles in the system DEM also solves the conservation of momentum and angular momentum for each particle. Conservation of energy equations are solved to resolve the temperature of both the continuous and discrete phase.

Some of the common models used to compute the fluid flow field and track the motion and energy of the particles are described below, these models are available to use in all the commercial software that can model the fluid using Eulerian approach and particles using Lagrangian model.

3.2.1 Flow and energy models:

Laminar model is used when the velocity of the fluid is known and the fluid never transitions into turbulent flow. Turbulent flow model can be used at high Reynolds number flows, but in most of the cases the fluctuations in the flow are small and it is not desirable to resolve them due to the high computational resources required (Cd-Adapco, 2016). Therefore, instead of solving the turbulent flow governing equations, Reynolds averaged Navier-Stokes (RANS) models (Zhai et al., 2007) and Scale – resolving simulations (Zhai et al., 2007) (using Large eddy simulation or Detached Eddy simulation) implementations are used .

Segregated flow and energy models are used which solves the conservation equations of mass, momentum and energy sequentially. This formulation also scales linearly with the cell count, so convergence is not deteriorated even if the mesh is refined (Cd-Adapco, 2016). The equations solved by the flow and energy model are described below (Norouzi et al., 2016), these are volume averaged over a fluid cell.

Continuity equation (conservation of mass)(Norouzi et al., 2016):

$$\frac{\partial\left(\rho_f \varepsilon_f \boldsymbol{u}\right)}{\partial t} + \nabla . \left(\rho_f \varepsilon_f \boldsymbol{u}\right) = 0 \tag{1}$$

Navier-Stokes equation (conservation of Momentum)(Norouzi et al., 2016):

$$\frac{\partial(\rho_f \varepsilon_f \boldsymbol{u})}{\partial t} + \nabla . \left(\rho_f \varepsilon_f \boldsymbol{u}\boldsymbol{u}\right) = -\frac{1}{\rho}\nabla p - \nabla . \boldsymbol{\tau}_f + \rho_f \varepsilon_f g - \boldsymbol{F} \tag{2}$$

Where ρ_f is the fluid density, ε_f is the volume fraction of fluid in the cell. $\boldsymbol{u}$ is the average velocity of the fluid, $\boldsymbol{\tau}_f$ is the fluid phase stress tensor, $\boldsymbol{F}$ is the volumetric mean of all the forces acting on the particle by the surrounded fluid in a fluid cell, which include the drag force, fluid pressure force, shear stress forces

Conservation of energy equation(Norouzi et al., 2016):

$$\frac{\partial(\rho_f \varepsilon_f C_{p,f} T_f)}{\partial t} + \nabla.[\boldsymbol{u}\varepsilon_f \rho_f C_{p,f} T_f] = \nabla.(\varepsilon_f k_f \nabla \mathrm{T}_f) + E_f \quad (3)$$

Where, $C_{p,f}$ is the specific heat capacity of fluid, T_f is the temperature of the fluid, k_f is the thermal conductivity of the fluid, E_f is the net rate of heat transferred to the fluid per unit volume, which includes rate of heat exchanged between fluid and particles, fluid and wall, heat generated through friction and from viscous forces.

3.2.2 Lagrangian multiphase model:

This model allows the use of dispersed phases in the physics continuum which is a continuous phase whose governing equations are in Eulerian form (equations 1, 2 & 3). The dispersed phases are modeled as parcels and tracked through the continuum. These dispersed phases are called Lagrangian phases and additional models can be applied to these phases. The dispersed phase particles are modeled as soft spheres by using the DEM particles model. As described in the section 2.2, Newton's equations of motion are used to model the motion of the particles in space and time. Therefore, it is important to identify all the external forces acting on the particles in the system to accurately model the motion of the particles. The external forces acting on the particles in fluid - particle system are drag force by the fluid, gravity, buoyancy force, contact forces between particles and contact force between particles and surroundings (walls).

For Solid Phase(Sen et al., 2014):

$$m_i \frac{dv_i}{dt} = F_{total} \quad (4)$$

$$F_{total} = \sum F_{contact} + \sum F_{external} \quad (5)$$

Where m_i, v_i are the mass and velocity of the ith particle. F_{total} is the net force on the particle which is the sum of particle – particle, particle – wall contact forces and external forces acting on the particles such as gravity, drag force by the fluid, buoyancy force.

Conservation of energy for solid phase(Cd-Adapco, 2016):

$$m_i C_{p,i} \frac{\partial T_i}{\partial t} = E_p \tag{6}$$

Where,m_i, T_i are the mass and temperature of the ith particle, $C_{p,i}$ is the specific heat capacity of the material, E_p is the net rate of energy transfer from the fluid.

3.2.3 Contact forces and External force models:

The net force acting on the particles is the sum of contact forces (particle – particle and particle – wall contact) and external forces (gravity, drag force). The following models are used to calculate the forces on the particles.

Contact forces: To model the normal and tangential components of the contact forces, Hertz – Mindlin No slip contact model [(Di Renzo and Di Maio, 2004), (Johnson, 1985)] has been used. This model uses equivalent radii and mass in its formulation as shown below (Cd-Adapco, 2016),

$$R_{eq} = \frac{1}{\frac{1}{R_a} + \frac{1}{R_b}} \tag{7}$$

$$M_{eq} = \frac{1}{\frac{1}{M_a} + \frac{1}{M_b}} \tag{8}$$

Where R_a, R_b are the radii of the colliding particles and M_a, M_b are the masses of the colliding particles. To calculate the contact forces for the particle – wall interaction, the

same model has been used with radius and mass of the wall being infinite (far greater than the particle radius and mass).

External forces: Gravity model is used to account for the weight of the particles. To model the drag forces in a high density solid systems, such as fluid beds, Gidaspow drag model is used. Gidaspow model described below, is a combination of Wen Yu and Ergun equations to calculate the drag coefficient [(Cd-Adapco, 2016), (Gidaspow, 1994)].

$$C_d = \frac{4}{3}\left(150\frac{1-\vartheta_f}{\vartheta_f R_p} + 1.75\right) \qquad if\ \vartheta_f < \vartheta_{min} \tag{9}$$

Otherwise

$$C_d = \frac{(24 + 3.6 * R_p^{0.687})}{R_p} * \vartheta_f^{-3.65} \tag{10}$$

Where, ϑ_f is the void fraction and ϑ_{min} is the minimum void fraction and R_p is the particle Reynolds number.

Energy Transfer through conduction during particle – particle interaction and particle – boundary interaction is modeled using following equation (Cd-Adapco, 2016),

$$q_{ab} = 4 * r_c * k * (T_a - T_b) \tag{11}$$

3.2.4 Implicit unsteady state model

Implicit unsteady model is used to model time. In this model, each CFD time step has inner iterations which are determined by observing the effect of it on the convergence. The CFD time step for the simulations was set at 2E-4 and only 1 inner iteration is used as the residuals were fairly low and convergence is seen. Any increase in inner iterations would increase the computational load and thereby increasing the total solver time. If the residuals are not low or not converging, a higher number of inner iterations or a lower

CFD time step should be preferred. DEM time step is calculated as a fraction of Rayleigh time (Cd-Adapco, 2016). Alternatively, a user defined time step can be used.

3.2.5 Lagrangian Passive scalar model

One of the objectives of this thesis is to study the effect of inlet air volumetric flow rate on the particle residence time distribution inside the spray zone. To achieve this a passive scalar model is used. Passive scalar model is analogous to tracer dyes used to measure fluctuations in concentration or velocity in a fluid flow. A passive scalar source term is added to the particles by defining a function such that the passive scalar model colors/tags the particles with their residence time inside the spray zone. If a particle stays inside spray zone for 10 iterations, then the passive scalar model tags that particular particle with a residence time of 10* DEM time step. Using such a function, the residence time of the particles inside the spray zone can be calculated. The passive scalar model does not affect the properties of the particles (Cd-Adapco, 2016).

3.3 Simulation properties

The fluidization of the particles is classified into four groups based on the difference between particle, fluid densities and the particle mean size (Geldart, 1973). Through Geldart's classification, it can be seen that the powders which fall under group A and group B are common types of powders and easy to fluidize. Powders which fall under group A and group B fluidize at minimum fluidization and there is a moderate to high mixing in these powders (Rhodes, 2008). Powders in group C are too cohesive to fluidize and powders in group D are too large and spout relatively easily even in deep beds. The particle size of the powders in group B are in the range of 150 to 1000 microns (Cocco et al., 2014). In the current CFD – DEM framework, particles of diameter 1 mm and density of 1460 kg/m^3 has been used (Group B particles).

3.3.1 Scaling of the system using similarity models:

In the current model, particles of diameter of 1 mm are considered with a batch size of 2 kg. The total number of particles in this system is 2.6 million. Simulating a system with 2.6 million particles is computationally expensive and impractical. The computational load increases quadratically with the increase in number of particles. Link et al. (Link et al., 2009) found good qualitative agreement between the experiments and the simulations by keeping the minimum fluidization velocity, Particle Reynolds number and Archimedes number as constants while scaling the system. Similar scaling model has been adapted by Börner et al. (Börner et al., 2016) and their experimental results (PIV images) agree with the particle hydrodynamics in the scaled systems. We have used this similarity scaling approach to scale our system by keeping the minimum fluidization velocity, particle Reynolds number and the Archimedes number constant. The minimum fluidization velocity (U_{mf}) has been calculated by rearranging the Ergun equation in terms of Archimedes and particle Reynolds number (Rhodes, 2008). The mathematical equations for U_{mf}, Archimedes number (Ar) and particle Reynolds number (for low Reynolds number) ($@U_{mf}$)(Re_{mf}) are described by equations 12, 13 and 14(Rhodes, 2008) respectively.

$$U_{mf} = \frac{Re_{mf} * \gamma}{\rho_g * d_p} \tag{12}$$

$$Ar = \frac{g * d_p^3 * (\rho_p - \rho_g)}{\gamma^2 * \rho_g} \tag{13}$$

$$Re_{mf} = (28.7^2 + (0.0494 * Ar))^{0.5} - 28.7 \tag{14}$$

To keep the U_{mf}, Ar and Re_{mf} as constants, particle density, gas density and kinematic viscosity of gas are scaled according to the scaling factor $k = \frac{d_{p2}}{d_{p1}}$. Where, d_{p2} is the particle diameter in the scaled system and d_{p1} is the particle diameter in the original system.

The particle and gas properties of original and the scaled system are presented in Table 3.3. The system is scaled to 4 times the actual size to reduce the computational load of the simulation but also making sure that the grid size for CFD is small enough to get an accurate solution. In a coupled CFD – DEM simulation, the base size of the mesh should be greater than that of the particle.

Parameter	***Original***	***Scaled***	***units***
Number of Particles	2616246	40780	[-]
Scaling factor (k)	1	4	[-]
Particle diameter (d_p)	0.001	0.004	m
Particle density (ρ_p)	1460	366	kg/m^3
Gas viscosity (γ)	1.85E-05	7.40E-05	m^2/s
Mass of the bed	2	0.5	kg
Gravity (g)	9.8	9.8	m/s^2
Gas density (ρ_g)	1.18415	1.18415	kg/m^3
Minimum fluidization velocity(Umf)	0.343	0.343	m/s
Archimedes number (Ar)	35275.76	35275.76	[-]
Reynolds number (Re$_{mf}$) @ U$_{mf}$	21.96	21.96	[-]

Table 3.3. Particle and gas properties for the original and scaled system.

3.3.2 Boundary and operating conditions for simulation setup

To study the effect of process parameters (air flow rate and temperature) on the process dynamics and the particle residence times inside the spray zone, three inlet volumetric flow rates of 80 m^3/h, 110 m^3/h and 130 m^3/h with temperatures of 30 ^oC and 50 ^oC are chosen. A total of six simulations were performed. The design space is presented in table 3.4.

Volumetric flow rate of Air (m^3/h)	***Mass flow rate of Air (kg/s)***	***Temperature(^oC)***
80	0.0263	30 ^oC
80	0.0263	50 ^oC
110	0.0362	30 ^oC
110	0.0362	50 ^oC
130	0.0428	30 ^oC
130	0.0428	50 ^oC

Table 3.4. Design space for the simulations.

The volumetric flow rates and temperatures are taken from the experiments performed using a GPCG system at BMS.

The boundary condition at the domain inlet is specified by the mass flow rate value (suggested boundary condition by STAR-CCM+) and at the domain outlet, the gauge pressure is set to 0 Pa. The boundary conditions at walls are set to no-slip conditions.

The initial conditions for air and inside the domain is set to an initial velocity of 0 m/s and an initial temperature of 293.15 k. The particles are initially allowed to settle without any inlet air flow, once the kinetic energy of the particles go to zero, air flow is then started to allow the particle bed to fluidize.

4. Results and Discussion

The two way coupled CFD – DEM model developed is studied at three different air flow rates corresponding to 4, 5.4 and 6.4 times the minimum fluidization velocities (Table 4) at air temperatures of 30 ^{o}C and 50 ^{o}C. The simulations were run for 10 seconds. A good convergence of CFD solution is achieved as the residual values have gone down 2 orders of magnitude. As mentioned in section 3.1.1, the fluid bed is divided into bottom and top compartment. The bottom compartment is demarcated by the end of the spray zone, the remaining geometry is the top compartment, which contains the spray zone. This demarcation is used to compare the results in the top compartment and the bottom compartment.

Average particle velocities, temperatures, number of collisions between particles in both top and bottom compartments, average fluid velocities and temperatures are saved at every 0.005 seconds of simulation. An internal interface has been placed between the bottom and the top compartment to monitor the number of particles transferring between the top and the bottom compartment.

Using passive scalar model, the residence time of the particles inside the spray zone has been calculated.

4.1 Effect of inlet air flow rate and temperature on the particle dynamics

4.1.1 Effect on Particle velocities

Increase in inlet air flow rates increased the average particle velocities in both the compartments and the temperature also followed a similar trend with increasing inlet air flow rate. This is because increase in air flow rate provides a higher transfer in momentum and energy from the fluid phase to solid phase.

Figure 4.1 shows the comparison of time averaged particle velocities in the bottom and top compartments for the three volumetric flow rates. The particles in top compartment have a higher velocity as expected as there are far few collisions in the top of the compartment

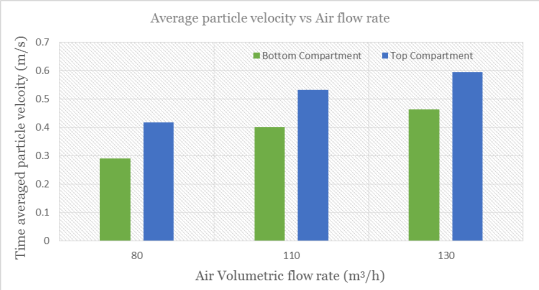

Figure 4.1. Time averaged particle velocity in both compartments at different inlet air flow rates.

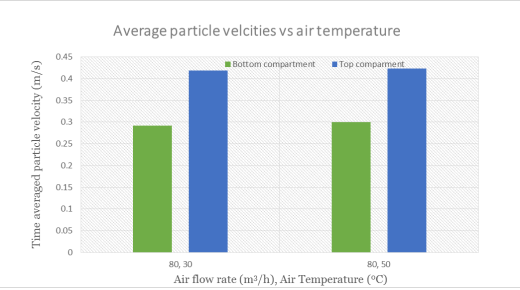

Figure 4.2. Time averaged particle velocity in both compartments at different inlet air temperatures.

due to the tapered shape and particles are closer together in the bottom compartment of the fluid bed leading to more collisions and low velocities.

The change in temperature should not have an effect on the particle velocities, it can be seen in Figure 4.2 that the time averaged particle veocities are similar for the inlet air flow rate of 80 m^3/h at air temperatures of 30 and 50 ^oC. The is true across the different inlet air flow rates at two different inlet air temperatures. This shows the reproducability of the simulations.

In Figure 4.3, the instantaneous particle velocities figures at different volumertic flow rates at 2 and 10 seconds of simulation time are presented. The color blue represents low velocity particles and color red represents high velocity particles. The geometry is sliced through the X-Z plane to get a better view at the fluidization of particles and also bubbles formed by the flow air through the particle bed.

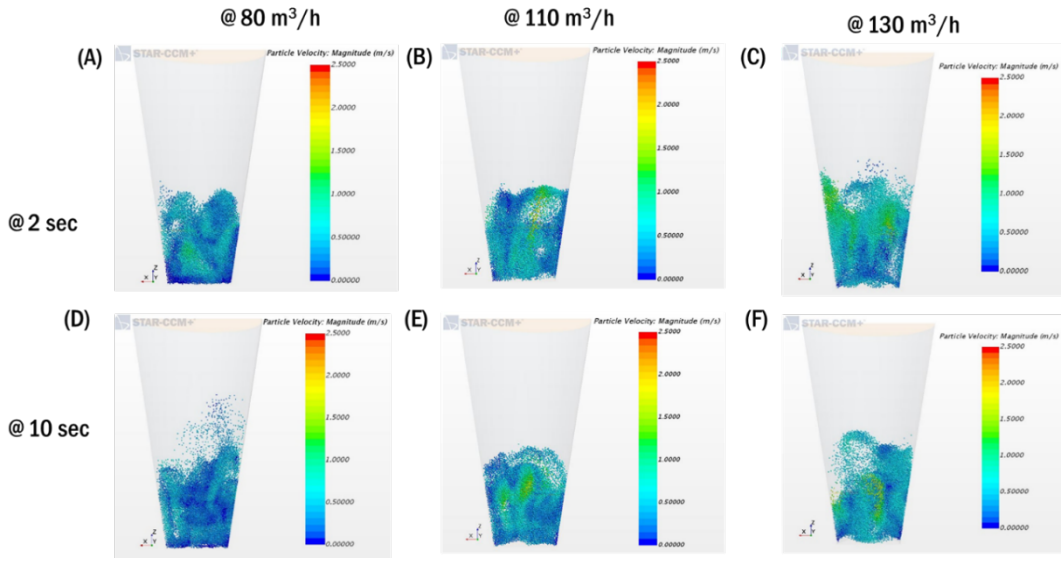

Figure 4.3: Instantaneous particle velocities. The domain is sliced along the x-z plane to get a better view of fluidization. (A) V = 80 m^3/h, t = 2 sec (B) V = 110 m^3/h, t = 2 sec (C) V = 130 m^3/h, t = 2 sec (D) V = 80 m^3/h, t = 10 sec (E) V = 110 m^3/h, t = 10 sec (F) V = 130 m^3/h, t = 10 sec. (V = air flow rate)

4.1.2 Effect on particle temperatures

The particle temperature increases with increasing inlet air flow rate as well as increasing air temperatures because of higher heat flux transferring from air to the particles. Figure 4.4 shows the average particle temperature over time in the bottom compartment, with inlet air temperatures of 30 ^oC, the average temperature changes about 1.5% – 2%. Figure 10 shows the average particle temperature over time in the bottom compartment, with inlet air temperatures of 50 ^oC, the average temperature changes about 4.3% – 5.6%.

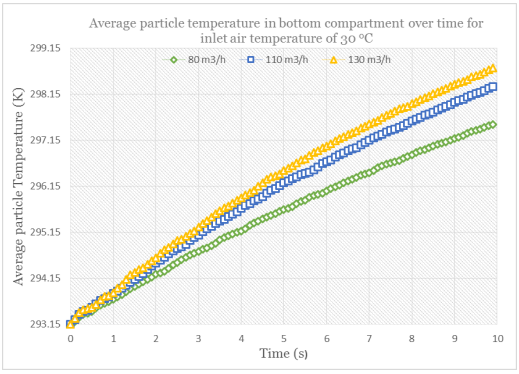

Figure 4.4. Average particle temperatures in the bottom compartment over time at different air flow rates at T= 30 °C

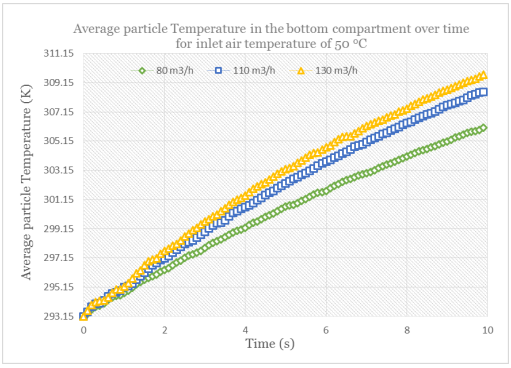

Figure 4.5. Average particle temperatures in the bottom compartment over time at different air flow rates at T= 50 °C

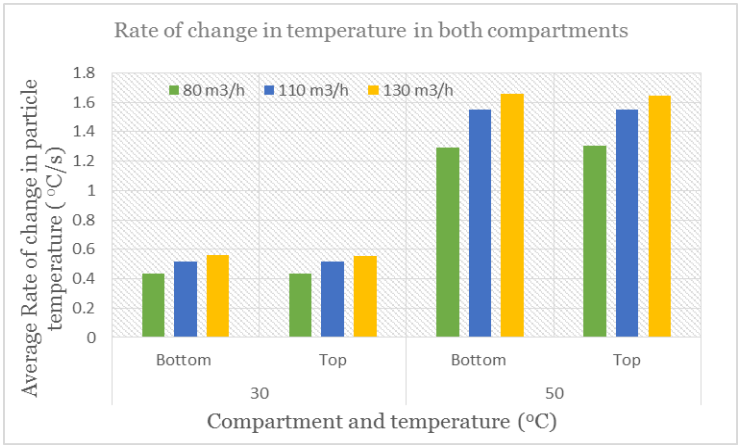

Figure 4.6. Average Rate of change in particle temperatures.

Figure 4.6 shows the rate of change in average particle temperatures in both bottom and top compartments for all the inlet air flow rates and air temperatures. The particles in both compartments reach similar levels of temperature and particles in the top compartment heat up at a slightly lower rate for both the temperature levels of 30 and 50 °C as the air that enters the top compartment is relatively cooler than that enters the bottom compartment. Which indicates that the inlet air flow rate at or above 80 m^3/h doesn't cause differences in temperatures in the bottom and the top compartment possibly due to good contact between air and the particles and good circulation of particles between the bottom and the top compartments. It can be seen that at air temperature of 50 °C, the

particles get heated up much faster (about 3 times) than at 30 ^{o}C, this is because the rate of heat transfer is directly proportional to temperature difference between air and particles.

4.1.3 Effect on collision frequency and circulation of particles

In wet granulation process, particles collide with each other and depending upon the collision velocities and the amount of liquid present on the surface of the particles, agglomeration or breakage of particles occur. To mechanistically calculate the rate processes of agglomeration, breakage and consolidation in granulation, collision frequency and collision efficiency data should be obtained from the CFD – DEM model (Sen et al., 2014).

From this model, number of collisions between particles in both the compartments are extracted from the simulations. The collision frequency is calculated as the number of collisions/ (No. of particles^2 * Δt). Figure 4.7 shows the average collision frequency in the bottom compartment at different inlet flow rates, average collision frequency in bottom is greater than that in the top compartment, the collision frequency in the bottom compartment is not effected significantly by the air flow rate as the particles in the bottom compartment are closer together in all the cases. Figure 4.8 shows the average collision frequencies in the top Compartments for three different inlet air flow rates. The collision frequency of particles decrease with the increase in air flow rate. Because of the higher particle velocities in case of high air flow rates, particles move away from each other resulting in lower number of collisions.

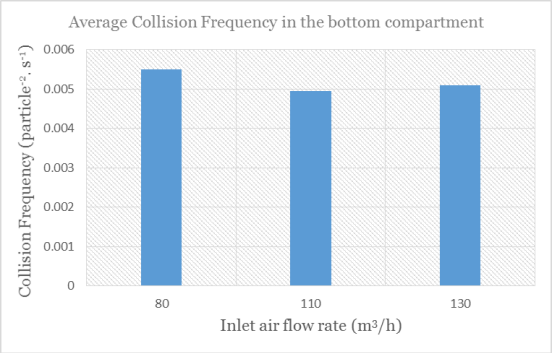

Figure 4.7. Average Collision frequency in the bottom compartment.

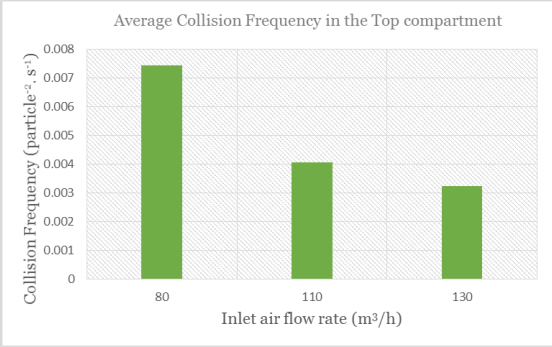

Figure 4.8. Average Collision frequency in the Top compartment.

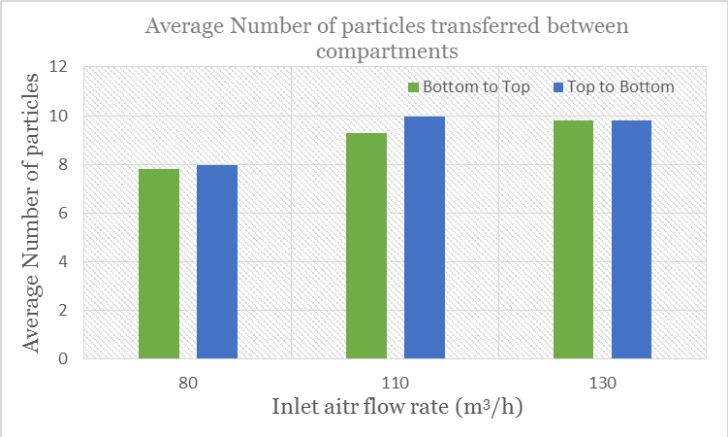

Figure 4.9. Average Number of particles transferred between compartments

To study the circulation of particles from one compartment to the other, an internal interface was created (virtual and does not affect the simulation) and the particles passing through that interface were tracked.

In Figure 4.9 average number of particles transferred between bottom and top compartment and vice-versa for inlet air flow rate of 80 m^3/h, 110 m^3/h and 130 m^3/h are shown, the transfer of particles between the bottom to top compartments increase with increasing air flow rate because of higher particle velocities. This indicates lower turnover rate of particles in case of lower flow rates.

4.2 Effect of inlet air flow rate on the particles residence time in Spray zone

The wetting of powder particles with liquid binder cannot be directly simulated using the current setup. Instead of particle wetting, residence time of particles inside the spray zone is calculated by incorporating a passive scalar model (section 3.1.5). The model, using a user defined function, calculates the residence time of particles inside the spray zone.

The residence time of the particles inside the spray zone would represent wetting here, the longer the particle stays inside the spray zone, more liquid binder is added to the particle. At the end of the 10 sec, homogenous distribution of particle residence time is expected which would indicate good mixing and circulation of particles from bottom to the top compartment and vice-versa (spray zone is in the top compartment).

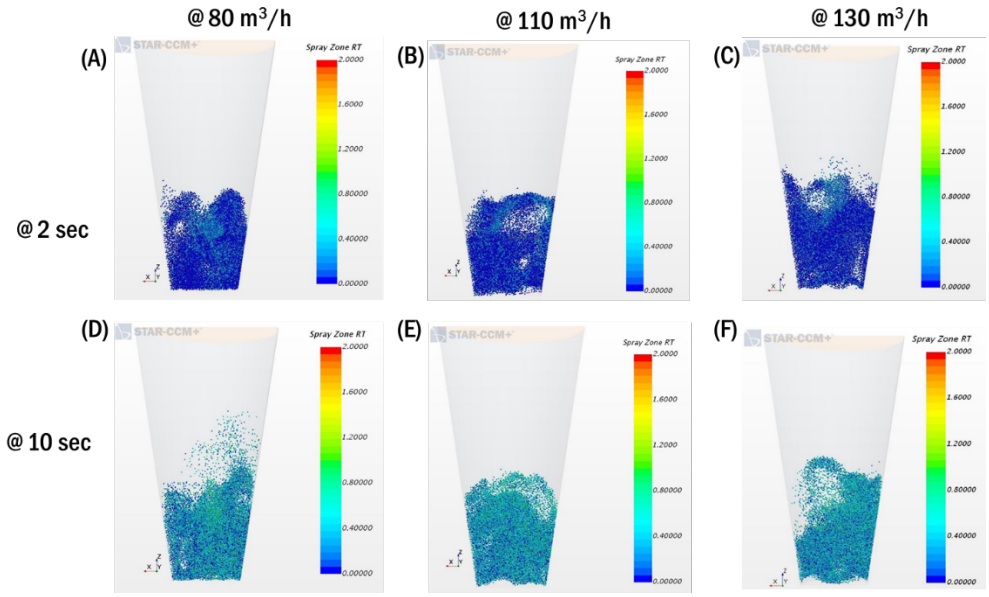

Figure 4.10. Particle residence time in spray zone at (A) V = 80 m³/h, t = 2 sec (B) V = 110 m³/h, t = 2 sec (C) V = 130 m³/h, t = 2 sec (D) V = 80 m³/h, t = 10 sec (E) V= 110m³/h, t= 10sec (F) V = 130 m³/h, t = 10sec.

Figure 4.10 shows the instantaneous residence time of the particles inside the spray zone for different inlet air flow rates at 2 and 10 seconds. At 2 seconds, the particles in the top compartment spend more time inside the spray zone than the particles in the bottom

compartment. At the end of the simulation (10 seconds) the wetting is much more homogenous in both the compartments and the particles in pictures E (110 m^3/h) and F (m^3/h) look more homogenous than those in picture D (80 m^3/h).

Residence time distributions of particles inside the spray zone are used to see whether the wetting is homogenous or not. Figure 4.11 shows the residence time distributions at 2, 5 and 10 seconds (end point) at an air flow rate of 110 m^3/h. The distribution is represented by ratio of number of particles to the total number of particles on the y-axis and residence time in spray zone (seconds) on the x-axis. The residence time distribution at 2 seconds shows that 40% of the bed did not go into the spray zone and the distribution moves towards the right as the time progresses. Finally at 10 sec distribution of residence time inside the spray zone shows that all the particles went into the spray zone with an average residence time of 0.3 sec. If the simulation were to run longer, the distribution at the end would resemble a Gaussian distribution. This distribution also shows that there is good

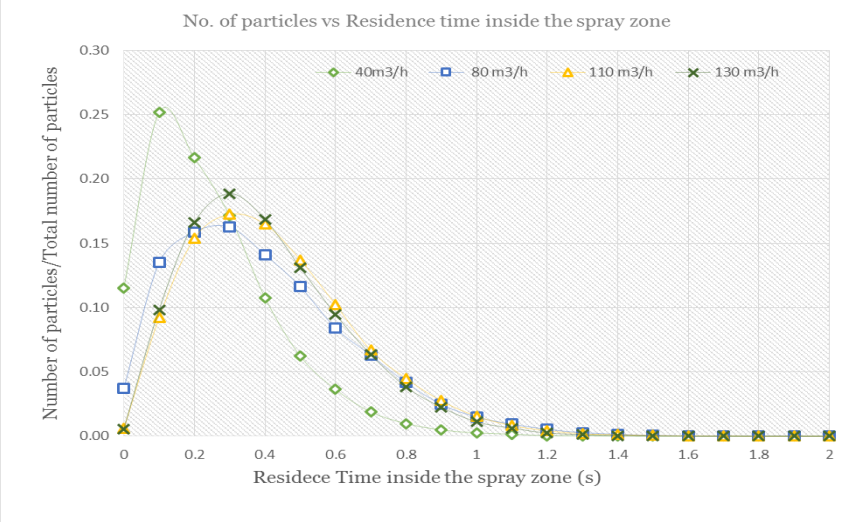

Figure 4.12. Particle residence time distributions inside the spray zone at different inlet air flow rates

circulation of particles from the bottom to the top compartment and vice versa for flow rate of 110 m^3/h.

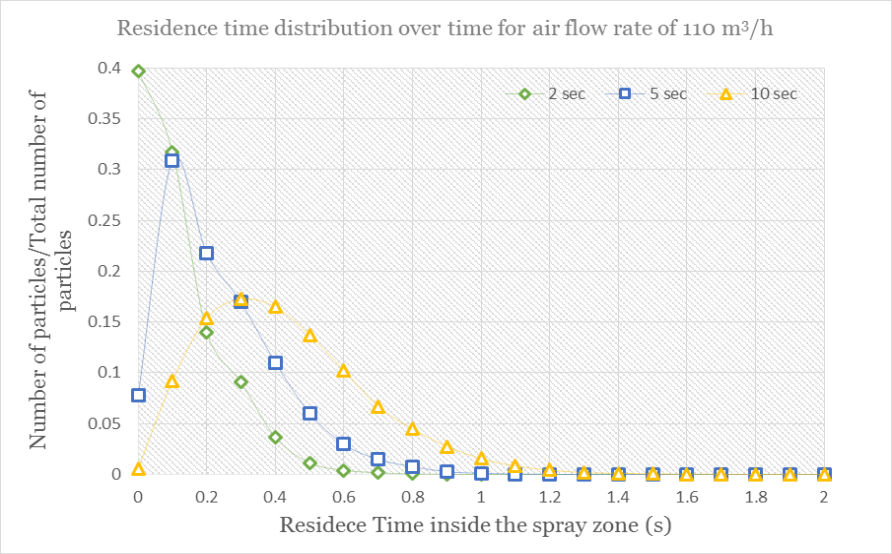

Figure 4.11 Residence time distribution inside the spray zone over time at an air flow rate of 110 m³/h

A simulation with low air flow rate (40 m³/h) was run to see the poor mixing and bad circulation of the particles between the bottom and the top compartment. Figure 4.12 shows the residence time distributions inside the spray zone for flow rates of 40, 80, 110 and 130 m³/h. For air flow rates 110 and 130 m³/h the distributions show that all the particles in the system spend time in the spray zone. Increase in air flow rate from 110 to 130 m³/h did not have a significant effect on the distribution, indicating that flow rate of 110 m³/h and above provide high intensity of fluidization and mixing in the granulator. For the air flow rate of 40 m³/h, the residence time distribution shows that 12% of the particles did not enter the spray zone suggesting that the particles did not fluidize well enough increasing the inlet flow rate to 80 m³/h decreased this to 4% suggesting a better fluidization. To get a better liquid distribution, flow rates above 80 m³/h should be used.

5. Conclusions

A two – way coupled CFD – DEM model is developed for a top spray fluid granulator has been developed by using STAR-CCM+. The effect of process parameters such as inlet air velocity and temperature on the particle dynamics and residence time of particles inside the spray zone were studied. The model was able to predict the changes in particle velocities, temperatures, collision dynamics and particle transfer from one compartment to the other as the inlet velocity and the temperature of the air changes. The collision frequency between the particles decreased with increasing air flow rate as the particles move away from each other as the air flow rate increases. This trend is seen in both the compartments. This mechanistic data can be used to determine the agglomeration rates in a granulation process.

From the particle residence time distribution inside the spray zone studied at different air flow rates, it was seen that at lower flow rates (40, 80 m^3/h), air does not fluidize the bed well enough, at the end of the 10 seconds of simulation, 12% and 4% of the particles did not go into the spray zone respectively. In case of higher flow rates, 110 and 130 m^3/h, particles spent more time in the spray and all of the particles go into the spray zone. The residence time distribution of particles for the air flow rates of 110 and 130 m^3/h are similar indicating that for flow rates above 110 m^3/h provide high fluidization and circulation of particles between the bottom and top compartments.

This multiscale multiphase framework provides important mechanistic data that can be used to develop hybrid CFD-DEM-PBM that describe the rate processes in granulation and understand the effect of process parameters on the product quality attributes.

References

Bokkers, G.A., Van Sint Annaland, M., Kuipers, J.A.M., 2004. Mixing and segregation in a bidisperse gas-solid fluidised bed: A numerical and experimental study. Powder Technol. 140, 176–186.

Börner, M., Bück, A., Tsotsas, E., 2016. DEM-CFD investigation of particle residence time distribution in top-spray fluidised bed granulation. Chem. Eng. Sci. 161, 187–197.

Burggraeve, A., Monteyne, T., Vervaet, C., Remon, J.P., Beer, T. De, 2013. Process analytical tools for monitoring, understanding, and control of pharmaceutical fluidized bed granulation: A review. Eur. J. Pharm. Biopharm. 83, 2–15.

Cameron, I.T., Wang, F.Y., Immanuel, C.D., Stepanek, F., 2005. Process systems modelling and applications in granulation: A review. In: Chemical Engineering Science. pp. 3723–3750.

Cd-Adapco, 2016. STAR-CCM+ v11.06.010 Documentation.

Chen, H., Liu, X., Bishop, C., Glasser, B.J., 2016. Fluidized Bed Drying of a Pharmaceutical Powder: A Parametric Investigation of Drying of Dibasic Calcium Phosphate. Dry. Technol. Just Accepted.

Cocco, R., Karri, S.B.R., Knowlton, T., 2014. Introduction to fluidization. Chem. Eng. Prog. 110, 21–29.

Cundall, P.A., Strack, O.D.L., 1979. A discrete numerical model for granular assemblies. Géotechnique 29, 47–65.

Di Renzo, A., Di Maio, F.P., 2004. Comparison of contact-force models for the simulation of collisions in DEM-based granular flow codes. Chem. Eng. Sci. 59,

525–541.

Ding Jianmin, Gidaspow, D., 1990. A Bubbling Fluidization Model Using Kinetic Theory of Granular Flow. AIChE J. 36, 523–538.

Fries, L., Antonyuk, S., Heinrich, S., Dopfer, D., Palzer, S., 2013. Collision dynamics in fluidised bed granulators: A DEM-CFD study. Chem. Eng. Sci. 86, 108–123.

Fries, L., Antonyuk, S., Heinrich, S., Palzer, S., 2011. DEM-CFD modeling of a fluidized bed spray granulator. Chem. Eng. Sci. 66, 2340–2355.

Geldart, D., 1973. Types of gas fluidization. Powder Technol. 7, 285–292.

Gernaey, K. V, Cervera-Padrell, A.E., Woodley, J.M., 2012. A perspective on PSE in pharmaceutical process development and innovation. Comput. Chem. Eng. 42, 15–29.

Gidaspow, D., 1994. Multiphase flow and fluidization, Journal of Non-Newtonian Fluid Mechanics. Academic Press.

Hoomans, B.P.B., Kuipers, J.A.M., Briels, W.J., van Swaaij, W.P.M., 1996. Discrete particle simulation of bubble and slug formation in a two-dimensional gas-fluidised bed: A hard-sphere approach. Chem. Eng. Sci. 51, 99–118.

Johnson, K.L., 1985. Contact Mechanics, Cambridge University Press. Cambridge University Press.

Kuipers, J.A.M., Duin, K.J. van, Beckum, F.P.H. van, Swaaij, W.P.M. van, 1993. Computer Simulation of the Hydrodynamics of a Two-Dimensional Gas-Solid Fluidized Bed. Comput. Chem. Eng. 17, 839–858.

Link, J.M., Godlieb, W., Tripp, P., Deen, N.G., Heinrich, S., Kuipers, J.A.M., Schönherr, M., Peglow, M., 2009. Comparison of fibre optical measurements and discrete

element simulations for the study of granulation in a spout fluidized bed. Powder Technol. 189, 202–217.

Lyngberg, O., Bijnens, L., Geens, J., Marchut, A., Mehrman, S., Schafer, E., 2016. Applications of modeling in oral solid dosage form development and manufacturing. In: Methods in Pharmacology and Toxicology. pp. 1–42.

Norouzi, H.R., Zarghami, R., Mostoufi, N., Sotudeh-Gharebagh, R., 2016. Coupled CFD-DEM Modeling: Formulation, Implementation and Application to Multiphase Flows. John Wiley & Sons.

Rhodes, M., 2008. Introduction to Particle Technology, Chemical Engineering and Processing. John Wiley & Sons.

Sen, M., Barrasso, D., Singh, R., Ramachandran, R., 2014. A Multi-Scale Hybrid CFD-DEM-PBM Description of a Fluid-Bed Granulation Process. Processes 2, 89–111.

Wormsbecker, M., Pugsley, T.S., Tanfara, H., 2007. The Influence of Distributor Design on Fluidized Bed Dryer Hydrodynamics. 12th Int. Conf. Fluid. New Horizons Fluid. Eng. 814–822.

Yuu, S., Umekage, T., Johno, Y., 2000. Numerical simulation of air and particle motions in bubbling fluidized bed of small particles. Powder Technol. 110, 158–168.

Zhai, Z.J., Zhang, W., Zhang, Z., Chen, Q.Y., 2007. Evaluation of various turbulence models in predicting airflow and turbulence in enclosed environments by CFD: part 1 - Summary of prevalent turbulence models. Hvac&R Res. 13, 853–870.